Oxidative and Osmotic Stress Signaling in Tumor Cells Is Mediated by ADAM Proteases and Heparin-Binding Epidermal Growth Factor

Oliver M. Fischer, Stefan Hart, Andreas Gschwind,† Norbert Prenzel,‡ and Axel Ullrich*

Department of Molecular Biology, Max Planck Institute of Biochemistry, D-82152 Martinsried, Germany

Mammalian cells respond to environmental stress by activating a variety of protein kinases critical for cellular signal transmission, such as the epidermal growth factor receptor (EGFR) tyrosine kinase and different members of the mitogen-activated protein kinase (MAPK) family. EGFR activation by stress stimuli was previously thought to occur independently of stimulation by extracellular ligands. Here, we provide evidence that osmotic and oxidative stresses induce a metalloprotease activity leading to cell surface cleavage of pro-heparin-binding EGF (pro-HB-EGF) and subsequent EGFR activation. This ligand-dependent EGFR signal resulted from stress-induced activation of the MAPK p38 in human carcinoma cells and was mediated by the metalloproteases ADAM9, -10, and -17. Furthermore, stress-induced EGFR activation induced downstream signaling through the MAPKs extracellular signal-regulated kinases 1 and 2 and JNK. Interestingly, apoptosis induced by treatment of tumor cells with doxorubicin was strongly enhanced by blocking HB-EGF function. Together, our data provide novel insights into the mammalian stress response, suggesting a broad mechanistic relevance of a p38–ADAM–HB-EGF–EGFR-dependent pathway and its potential significance for tumor cells in evasion of chemotherapeutic agent-induced apoptosis.

Exposure of mammalian cells to different forms of environmental stress such as hyperosmolarity, oxidative agents, ionizing radiation, or UV light is known to activate a variety of cellular signal transduction cascades. Reactive oxygen species (ROS) have been implicated as major mediators of stress-induced signaling, and the uncontrolled production of ROS has been connected to cellular damage in pathophysiological disorders such as cancer (17, 27). Moreover, mammalian cells have to adapt to changes in their extracellular environment such as an increase in osmolarity, which would result in cell shrinkage if not counteracted by an increased synthesis of small molecules to equalize intra- and extracellular conditions (13).

Osmotic or oxidative stress stimuli trigger the autophosphorylation of a variety of receptor tyrosine kinases (RTKs) including the epidermal growth factor receptor (EGFR), which is particularly sensitive to stress-induced activation (29, 30, 39, 41). The EGFR controls a plethora of important biological responses including cell proliferation, differentiation, migration, and antiapoptotic signaling and has therefore been implicated in diverse human disorders (37). Both ligand-dependent and -independent mechanisms have been reported for stimulation of EGFR tyrosine kinase activity. Ligand-mediated receptor activation is initiated by binding of an EGF-like ligand such as EGF, heparin-binding EGF (HB-EGF), amphiregulin (AR), betacellulin, epiregulin, or transforming growth factor α (TGF-α) to the receptor's ectodomain. Subsequent dimerization triggers the receptor's intrinsic kinase activity,

catalyzing autophosphorylation on intracellular tyrosine residues (45). In contrast, ligand-independent receptor activation has been proposed to occur via inactivation of phosphotyrosine phosphatases through ROS-induced oxidation of a critical cysteine residue within their catalytic pocket (30). Inhibition of negative regulation then results in an equilibrium shift from the nonphosphorylated to the phosphorylated state of the RTK. In addition, ligand-independent receptor activation has been suggested to involve nonspecific clustering and internalization of the EGFR (41). Furthermore, cytoplasmic nonreceptor tyrosine kinases such as c-Src and JAK2 have been shown to phosphorylate the EGFR (3, 50, 53).

Tyrosine phosphorylation of the EGFR is also induced upon stimulation of various G protein-coupled receptors (GPCRs), a conserved signaling process known as EGFR signal transactivation (12). Activation of this pathway was originally attributed to an exclusively ligand-independent mechanism. However, Prenzel and colleagues demonstrated that EGFR signal transactivation occurs via metalloprotease-mediated processing of active EGF-like ligand precursors and the involvement of the extracellular matrix (38). Very recently, members of the ADAM family of metalloproteases were identified as the sheddases required for GPCR-induced proteolytic processing of pro-HB-EGF and pro-AR ligand precursors. Several members of this enzyme family, such as ADAM10, ADAM12, and ADAM17 (also known as tumor necrosis factor alpha-converting enzyme), could be implicated in this signaling process (1, 21, 54). Aberrant signal transmission involving ligand-dependent EGFR transactivation has been implicated in the progression of various human disorders, such as head and neck squamous cell carcinoma, cardiac and gastrointestinal hypertrophy, and cystic fibrosis (1, 22, 28, 32). Furthermore, ADAM9 has been shown to process pro-HB-EGF in response to protein kinase C activation upon phorbol ester treatment (23), while cleavage of pro-TGF-α, pro-HB-EGF, and proamphiregulin by

* Corresponding author. Mailing address: Department of Molecular Biology, Max Planck Institute of Biochemistry, Am Klopferspitz 18A, D-82152 Martinsried, Germany. Phone: 49-89-8578-2512. Fax: 49-89-8578-2454. E-mail: ullrich@biochem.mpg.de.
† Present address: Department of Immunology, Genentech, Inc., South San Francisco, CA 94080.
‡ Present address: U3 Pharma AG, 82152 Martinsried, Germany.

ADAM17 has also been reported (34, 36, 47) and was implicated in tumorigenesis in the case of TGF-α (5).

Besides RTK phosphorylation, environmental stress leads to the activation of mitogen-activated protein kinase (MAPK) signaling, which couples various extracellular stimuli to the activation of transcription factors in the nucleus. MAPK signal transduction cascades thereby control important processes such as proliferation, migration, differentiation, and stress responses (9, 25). Apart from activating transcription factors, the MAPKs extracellular signal-regulated kinases 1 and 2 (ERK1/2) and p38 can control transmembrane protein processing (15) by phosphorylating the intracellular domain of ADAM17 (14, 16). The mechanisms of MAPK activation by osmotic and oxidative stress have been intensely studied (31). Previous reports implicated the downregulation of antagonistic phosphatases as well as the regulation of scaffolding protein function in MAPK activation induced by stress agents (2, 13). Moreover, small G proteins have been demonstrated to play a role in the activation of MAPK by osmotic stress (13). The activation of MAPK by stress stimuli has severe consequences for the development and progression of human cancer, as increasing evidence implicates both ROS and stress-activated MAPKs such as p38 and JNK in cancer cell proliferation and susceptibility to apoptosis. Importantly, recent studies revealed that exposure to anticancer drugs triggers stress-induced signaling cascades (reviewed in reference 2). As the EGFR might be part of this drug-induced stress signaling, its cellular functions are likely to determine the therapeutic results.

The mechanisms of RTK and MAPK activation in response to oxidative and osmotic stress have been intensely studied, but so far, these regulatory pathways have been generally described as ligand-independent processes in human carcinoma cells. Recent advances in understanding the regulation of EGFR activation by ADAM metalloproteases prompted us to investigate the mechanisms of stress-induced EGFR and MAPK stimulation with respect to a potential involvement of EGF-like ligand processing.

In this report, we establish the proteolytic cleavage of pro-HB-EGF as the critical step for EGFR activation in response to osmotic or oxidative stress and identify members of the ADAM family of metalloproteases as components of this process. We further provide evidence that stress-induced EGFR triggers the activation of the ERK and JNK MAPKs, whereas EGFR activation itself depends on p38 activity, implicating this MAPK as an upstream activator of ADAM metalloproteases in the stress response of human carcinoma cells. Finally, we show that blockade of HB-EGF function strongly enhances tumor cell death upon exposure to the chemotherapeutic agent doxorubicin, which induces p38 activation. Our findings suggest a role of the p38-ADAM-EGFR pathway in the escape of tumor cells from chemotherapy-induced cell death.

MATERIALS AND METHODS

Cell culture, plasmids, and transfections. All cell lines (American Type Culture Collection, Manassas, Va.) were routinely grown according to the supplier's instructions. Transfections of Cos-7 cells were carried out using Lipofectamine (Invitrogen) according to the manufacturer's protocol. Briefly, for transient transfections in 6-cm-diameter dishes cells were incubated for 4 h in 2 ml of serum-free medium containing 20 μl of Lipofectamine and 2 μg of total plasmid DNA per dish. The transfection mixture was then supplemented with an equal volume of 20% fetal bovine serum, and 20 h later, cells were washed and cultured
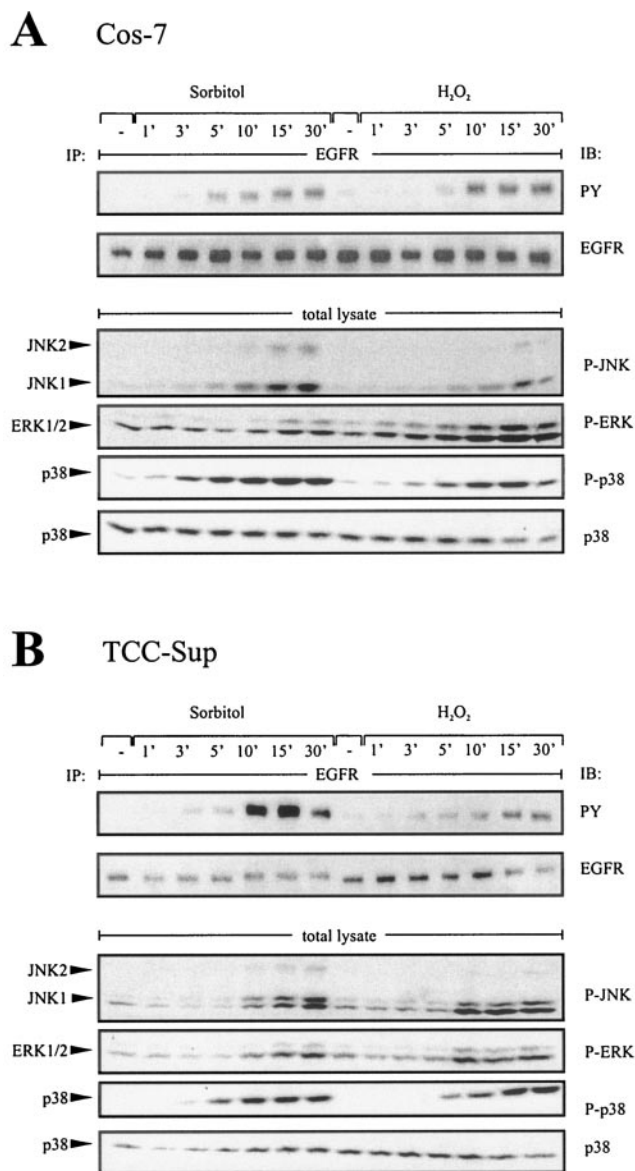

FIG. 1. Time course assay of stress-induced EGFR and MAPK phosphorylation in different cell lines. (A) EGFR and MAPK phosphorylation in response to osmotic and oxidative stress. Cos-7 cells were treated with sorbitol (0.3 M) and hydrogen peroxide (200 μM) for the indicated time periods. Following immunoprecipitation (IP) of cell extracts with anti-EGFR antibody, proteins were immunoblotted (IB) with antiphosphotyrosine antibody and reprobed with anti-EGFR antibody. Phosphorylated MAPKs were detected by immunoblotting total lysates with anti-phospho-ERK, anti-phospho-JNK, and anti-phospho-p38 antibodies. The same filters were reprobed with anti-p38 antibody. (B) Stress-induced EGFR phosphorylation in human bladder carcinoma cell lines. TCC-Sup cells were treated as indicated for panel A.

in serum-free medium for another 24 h prior to stimulation. The inhibitors AG1478 (Alexis Biochemicals), batimastat (BB94; British Biotech, Oxford, United Kingdom), Crm197 (Quadratech Ltd.), SB202190 (Calbiochem), and PD98059 (Alexis Biochemicals) were added to serum-starved cells before the respective stimulations. The plasmids pcDNA3-HA-ERK2 (11) and pcDNA3-pro-HB-EGF-VSV (38) were used in this study.
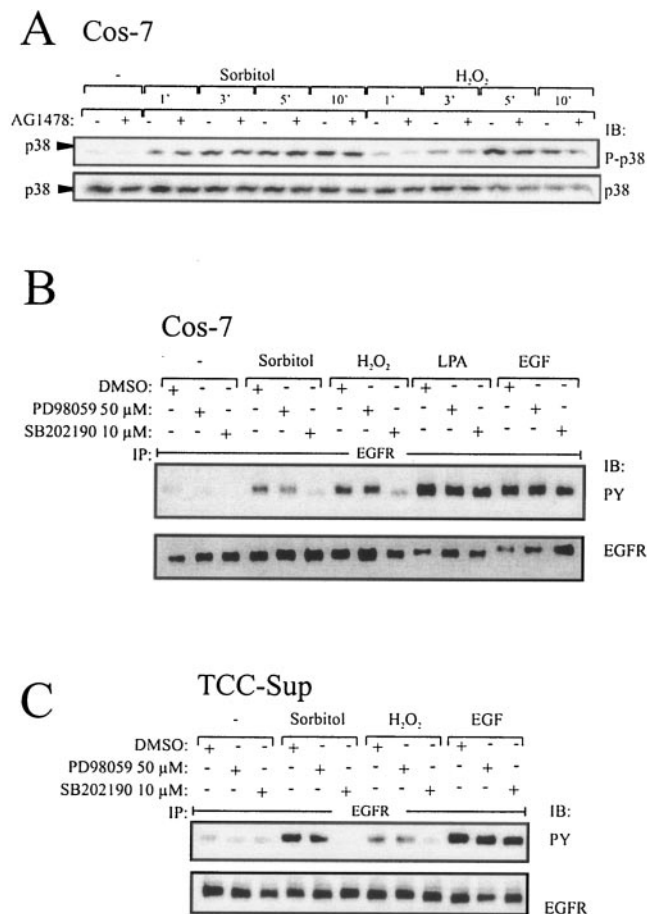
FIG. 2. p38 mediates stress-induced EGFR phosphorylation. (A) Time course assay of p38 phosphorylation dependent on EGFR kinase function. Cos-7 cells were pretreated with AG1478 (250 nM) or an equal volume of empty vehicle (dimethyl sulfoxide [DMSO]) for 20 min and stimulated with 0.3 M sorbitol or 200 μM hydrogen peroxide for the indicated periods. Cell extracts were immunoblotted with anti-phospho-p38 antibody, and the same filters were reprobed with polyclonal anti-p38 antibody. (B) Stress-induced EGFR activation depends on p38 but not ERK activity in Cos-7 cells. Cos-7 cells were pretreated with PD98059 (50 μM), SB202190 (10 μM), or an equal volume of empty vehicle (dimethyl sulfoxide) for 30 min and stimulated with 0.3 M sorbitol and 200 μM hydrogen peroxide for 10 min and the GPCR agonist LPA (10 μM) or EGF (2 ng/ml) for 3 min as a positive control. Cell extracts were assayed for EGFR tyrosine phosphorylation content. (C) Stress-induced EGFR activation depends on p38 activity in TCC-Sup carcinoma cells. TCC-Sup cells were pretreated as described for panel A and stimulated with 0.3 M sorbitol and 200 μM hydrogen peroxide for 10 min and EGF (2 ng/ml) for 3 min as a positive control. After lysis cell extracts were assayed for EGFR tyrosine phosphorylation content.

Protein analysis. Cells were lysed and proteins were immunoprecipitated as described before (11). Prior to lysis, cells grown to 80% confluence were treated with inhibitors and agonists as indicated in the figure legends and then lysed for 10 min on ice in buffer containing 50 mM HEPES (pH 7.5), 150 mM NaCl, 1% Triton X-100, 1 mM EDTA, 10% glycerol, 10 mM sodium pyrophosphate, 2 mM sodium orthovanadate, 10 mM sodium fluoride, 1 mM phenylmethylsulfonyl fluoride, and 10 μg of aprotinin/ml. Lysates were precleared by centrifugation at 13,000 rpm for 10 min at 4°C. Precleared lysates were immunoprecipitated using the respective antibodies and 20 μl of protein A-Sepharose for 4 h at 4°C. Precipitates were washed three times with 0.5 ml of HNTG buffer, suspended in 2× sodium dodecyl sulfate (SDS) sample buffer, boiled for 3 min, and subjected to gel electrophoresis. Following SDS-polyacrylamide gel electrophoresis, proteins were transferred to nitrocellulose membrane. Western blotting was per-

formed according to standard methods. The antibodies to human EGFR (108.1) and Shc have been characterized before (38). Phosphotyrosine was detected with the 4G10 monoclonal antibody (Upstate Biotechnology Inc., Lake Placid, N.Y.). Polyclonal anti-phospho-p44/p42 (Thr202/Tyr204) MAPK antibody and anti-phospho-JNK (Thr183/Tyr185) and anti-phospho-p38 (Thr180/Tyr182) antibodies were purchased from New England Biolabs (Beverly, Mass.). Polyclonal anti-ERK2, anti-JNK1, and anti-p38 antibodies were from Santa Cruz Biotechnology (Santa Cruz, Calif.). Polyclonal antibodies to ADAM10 and -17 were from Chemicon. The antibody to ADAM12 was provided by Beatrice Marg and was generated by immunization of rabbits with a fusion protein consisting of the extracellular domain of the protease aa 1 to 673 and an N-terminal GST tag. The polyclonal antibody against ADAM15 was produced against the peptide sequence CGTKSQGPAKPPPPKPL. Unless otherwise stated, the data shown are representative for three independent experiments. Quantification of Western blot experiments was performed using the Fuji LAS1000 system.

JNK activity assay. JNK activity was assayed as described previously (46). Cultured cells were lysed in lysis buffer containing 20 mM Tris (pH 7.6), 0.5% Nonidet P-40, 250 mM NaCl, 3 mM EDTA, 1 mM dithiothreitol, 0.5 mM phenylmethylsulfonyl fluoride, 20 mM β-glycerophosphate, 1 mM sodium orthovanadate, and 1 μg of leupeptin/ml. JNK was immunoprecipitated from lysates obtained from six-well dishes with polyclonal anti-JNK antibody. Immunoprecipitates were washed twice using lysis buffer and twice using kinase assay buffer (25 mM HEPES [pH 7.5], 20 mM β-glycerophosphate, 20 mM p-nitrophenylphosphate, 20 mM MgCl$_2$, 2 mM dithiothreitol, and 0.1 mM sodium orthovanadate). Kinase reactions were performed in 30 μl of kinase buffer supplemented with 1 μg of glutathione S-transferase (GST)–c-Jun (amino acids 1 to 79), 20 μM cold ATP, and 5 μCi of [γ-^{32}P]ATP at 30°C for 30 min. Reactions were stopped by addition of 30 μl of Laemmli buffer, and reaction mixtures were subjected to gel electrophoresis on 12.5% polyacrylamide gels. Labeled GST–c-Jun was quantitated using a phosphorimager (Fuji).

Flow cytometric analysis. Fluorescence-activated cell sorter analysis was performed as described before (38). In brief, cells were seeded, grown for 20 h, and serum starved for 24 h. Cells were treated with inhibitors and stimulated as indicated. After collection, cells were stained with an ectodomain-specific antibody to pro-HB-EGF for 45 min. After being washed with phosphate-buffered saline, cells were incubated with fluorescein isothiocyanate-conjugated secondary antibodies for 15 min and washed again with phosphate-buffered saline. Cells were analyzed on a Becton Dickinson FACScalibur flow cytometer.

TCA precipitation of HB-EGF. Cos-7 cells transiently transfected with pcDNA3-pro-HB-EGF-VSV were serum starved for 24 h. Prior to stimulation cells were washed, preincubated with BB94 (10 μM), and stimulated as indicated. After stimulation the supernatant was collected, sodium desoxycholate was added (100 μg/ml), and following incubation on ice for 10 min the solution was supplemented with trichloric acid (TCA) to a final concentration of 10% TCA. After incubation on ice for 30 min samples were centrifuged, the supernatant was discarded, and the precipitates were resuspended in Schägger-von Jargow sample buffer (4% SDS, 12% glycerol, 50 mM Tris-HCl [pH 6.8], 2% β-mercaptoethanol, 0.01% Serva Blue G) (44). TCA was neutralized using Tris-HCl (pH 8.8), and samples were separated using the Tricine-SDS gel electrophoresis protocol (44).

RNA interference and reverse transcription-PCR (RT-PCR) analysis. Transfection of 21-nucleotide small interfering RNA (siRNA) duplexes (Dharmacon Research, Lafayette, Colo.) for targeting endogenous genes was carried out using Oligofectamine (Invitrogen) for NCI-H292 cells and 4.2 μg of siRNA duplex per six-well plate as previously described (14a). Cos-7 cells were transfected using Lipofectamine 2000 (Invitrogen) according to the manufacturer's protocol. Briefly, 8.4 μg of siRNA duplex per 6-cm-diameter dish was incubated with 10 μl of Lipofectamine 2000 in 1 ml of serum-free medium for 20 min. The transfection mixture was added to the cell culture medium containing serum, and after 6 h, cells were washed and incubated in medium containing serum overnight. NCI-H292 and Cos-7 cells were serum starved and assayed 2 days after transfection. The highest efficiencies in silencing target genes were obtained by using mixtures of siRNA duplexes targeting different regions of the gene of interest. Sequences of siRNAs used were AAUCACUGUGGAGACAUUUGCdTdT and AAACUUCCAGUGUGUAGAUGCdTdT (ADAM9); AAUGAAGA GGGACACUUCCCUdTdT and AAGUUGCCUCCUCCUAAACCAdTdT (ADAM10); AACCUCGCUGCAAAGAAUGUGdTdT and AAGACCUUG AUACGACUGCUGdTdT (ADAM12); AACUCCAUCUGUUCUCCUGA CdTdT and AAAUUGCCACGCUGCGCCCGUCdTdT (ADAM15); AAA GUUUGCUUGGCACACCUUdTdT, AAGUAAGGCCCAGGAGUGUUd TdT, and AACAUAGAGCCACUUUGGAGAdTdT (ADAM17); and CGUA CGCGGAAUACUUCGAdTdT (control, GL2). The siRNA duplexes against ADAM12 and ADAM17 have been described earlier (21).
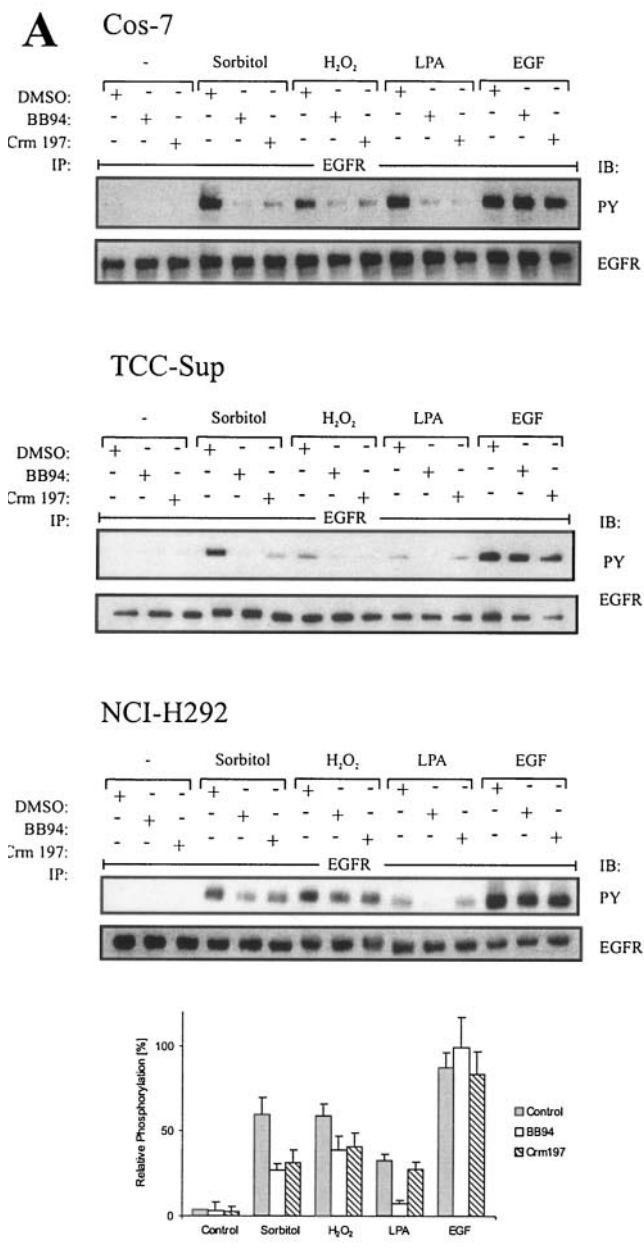
Specific silencing of targeted genes was confirmed by RT-PCR analysis. RNA isolated using the RNeasy Mini kit (Qiagen, Hilden, Germany) was reverse transcribed using avian myeloblastosis virus reverse transcriptase (Roche, Mannheim, Germany). PuReTaq Ready-To-Go PCR beads (Amersham Biosciences, Piscataway, N.J.) were used for PCR amplification. Primers (Sigma Ark, Steinheim, Germany) were as follows: ADAM9, 5′-AGT GCA GAG GAC TTT GAG AA-3′ and 5′-TGC CGT TGT AGC AAT AGG CT-3′; ADAM10, 5′-TTG CTC ACG AAG TTG GAC AT-3′ and 5′-TTT CCC AGG TTT CAG TTT GC-3′; ADAM15, 5′-GGC TGG CAG TGT CGT CCT ACC AGA GGG-3′ and 5′-GGT GCA CCC AGC TGC AGT TCA GCT CAG TCC-3′. PCR products were subjected to electrophoresis on a 2.5% agarose gel, and DNA was visualized by ethidium bromide staining.

Apoptosis assay. TCC-Sup bladder carcinoma cells were seeded, grown for 20 h, and treated with 10 μM doxorubicin and Crm197 (10 μg/ml) or BB94 (5 μM) as indicated for 72 h. Cells were collected in assay buffer containing propidium iodide and incubated at 4°C for 3 h. Nuclear DNA staining was analyzed on a Becton Dickinson FACScalibur flow cytometer.

RESULTS

Distinct kinetics of EGFR and MAPK activation in Cos-7 and human carcinoma cell lines. Osmotic or oxidative stress leads to both tyrosine phosphorylation of the EGFR and activation of MAPKs in a wide variety of cell systems (7, 13, 29). To investigate the underlying mechanisms, we performed time course experiments in Cos-7 and TCC-Sup bladder carcinoma cell lines and analyzed EGFR phosphorylation with phosphotyrosine-specific antibodies and MAPKs with activation-specific antibodies by immunoblot analysis. As shown in the upper panels of Fig. 1, tyrosine phosphorylation of the EGFR in response to the stress agents sorbitol (0.3 M) and hydrogen peroxide (200 μM) occurred in both cell lines within 5 to 10 min and thus preceded the activation of ERK and JNK MAPKs, which became phosphorylated after 10 and 15 min, respectively (Fig. 1A and B, lower panel). In stark contrast, phosphorylation of p38 occurred as an immediate response to stress agents. The results of these time course experiments were consistent with a role for p38 as an upstream mediator of EGFR activation and further pointed to a function of ERK1/2 and JNK as downstream effectors of the EGFR in response to stress stimuli.

p38 controls EGFR activation by osmotic and oxidative stress. The finding that p38 activation preceded EGFR tyrosine phosphorylation (Fig. 1) raised the question of whether p38 acts as an upstream regulator of EGFR stimulation in Cos-7 and human carcinoma cell lines.
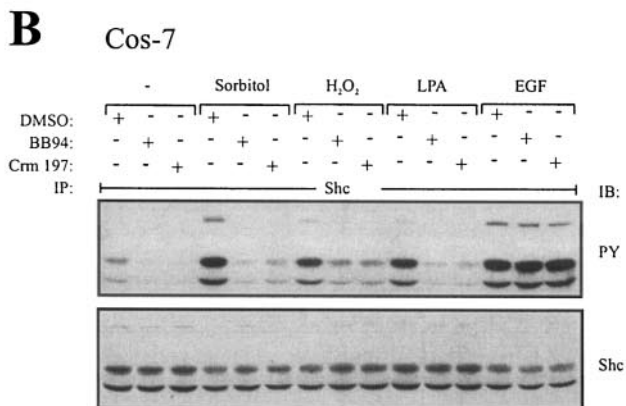
FIG. 3. EGFR activation in response to osmotic and oxidative stress is ligand dependent. (A) Effect of metalloprotease and HB-EGF inhibition on EGFR phosphorylation. Cos-7, NCI-H292, and TCC-Sup cells were serum starved for 24 h; pretreated with BB94 (10 μM), the diphtheria toxin mutant Crm197 (10 μg/ml), or an equal volume of empty vehicle (dimethyl sulfoxide [DMSO]) for 20 min; and stimulated for 10 min with 0.3 M sorbitol, 200 μM hydrogen peroxide, 10 μM LPA, or 2 ng of EGF/ml. Following immunoprecipitation of cell extracts with anti-EGFR antibody, proteins were immunoblotted with antiphosphotyrosine antibody and reprobed with anti-EGFR antibody. Data from three independent experiments were quantified with the Fuji LAS1000 imaging system. (B) Analysis of Shc phosphorylation in response to stress agents. Cos-7 cells were treated as described for panel A. After immunoprecipitation of Shc from cell extracts with a polyclonal anti-Shc antibody, proteins were immunoblotted with antiphosphotyrosine antibody and reprobed with anti-Shc antibody.
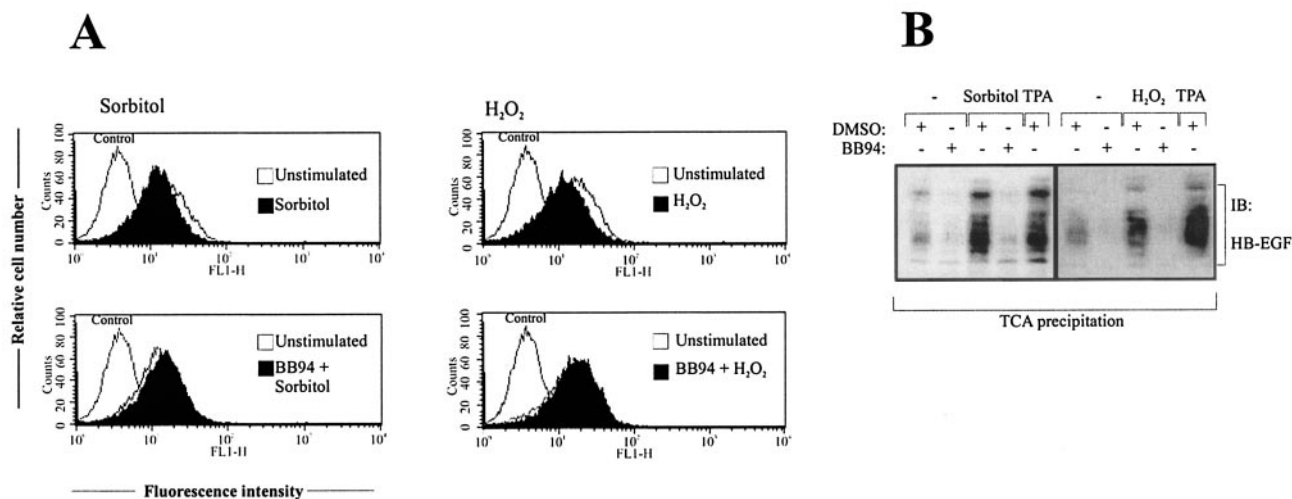
FIG. 4. Analysis of pro-HB-EGF release in response to stress agents. (A) Flow cytometric analysis of pro-HB-EGF processing. Cos-7 cells were pretreated with BB94 (10 μM) or an equal volume of empty vehicle (dimethyl sulfoxide [DMSO]) for 20 min and stimulated with 0.3 M sorbitol or 200 μM hydrogen peroxide for 30 min. Cells were collected and stained for surface pro-HB-EGF and analyzed by flow cytometry. Control cells were labeled with fluorescein isothiocyanate-conjugated secondary antibody alone. (B) Immunoblot analysis of conditioned media. Cos-7 cells were transiently transfected with pro-HB-EGF cDNA. After serum starvation for 24 h cells were stimulated for 20 min with sorbitol (0.3 M) or hydrogen peroxide (200 μM), and proteins within the supernatant medium were precipitated by TCA precipitation. Precipitated proteins were subjected to Tricine-SDS gel electrophoresis according to the protocol of Schägger and von Jargow and subsequent immunoblot analysis with anti-HB-EGF antibody. TPA stimulation has been included as a positive control. The data shown are representative of three independent experiments.

Preincubation of Cos-7 cells with the selective EGFR kinase inhibitor AG1478 did not affect p38 phosphorylation in response to stress agents (Fig. 2A), demonstrating that p38 activation was independent of EGFR activity. To address the question whether p38 is located upstream of the EGFR, we used the p38-specific inhibitor SB202190, which is frequently used to interfere with p38 function, to investigate the effect of inhibiting p38 activity on stress-induced EGFR activation. As shown in Fig. 2B, preincubation of Cos-7 cells with SB202190 completely eliminated stress-induced EGFR activation while leaving lysophosphatidic acid (LPA) and EGF-induced receptor phosphorylation unaffected. In contrast, the MEK1/2 inhibitor PD98059 did not affect EGFR phosphorylation. Analogous results were obtained with the bladder carcinoma cell line TCC-Sup (Fig. 2C). Taken together, these results implicate p38 as an upstream mediator of EGFR activation in the stress-induced signaling response of Cos-7 and TCC-Sup bladder carcinoma cells.

Stress-induced EGFR phosphorylation depends on metalloprotease activity and HB-EGF function. Recent investigations underscored the importance of EGF-like ligand precursor processing in EGFR phosphorylation upon stimuli such as GPCR signals (38). Based on these findings, we asked whether EGFR activation by stress stimuli may also involve a ligand-dependent mechanism. We therefore preincubated cells with the metalloprotease inhibitor batimastat (BB94), which has been shown to inhibit EGF-like ligand processing and subsequent EGFR transactivation (38). Upon stimulation with stress agents, EGFR tyrosine phosphorylation was monitored by immunoblot analysis with phosphotyrosine-specific antibody. As shown in Fig. 3A, BB94 almost completely blocked sorbitol or hydrogen peroxide-induced EGFR phosphorylation in Cos-7 and TCC-Sup bladder carcinoma cells (upper and middle panels).

In the lung carcinoma cell line NCI-H292, BB94 reduced EGFR activation by about 50%, suggesting an alternative parallel activation mechanism (Fig. 3A, lower panel).

Next, we investigated the effect of the diphtheria toxin mutant Crm197, a specific antagonist of HB-EGF function, on stress-activated EGFR tyrosine phosphorylation. Indeed, Crm197 inhibited EGFR phosphorylation to the same extent as did BB94, suggesting that HB-EGF is critically involved in stress-induced EGFR activation in the three cell lines tested. Control stimulations showed that EGFR tyrosine phosphorylation by LPA was completely prevented by both inhibitors while neither Crm197 nor BB94 affected direct receptor stimulation upon EGF treatment.

Furthermore, we investigated whether this ligand dependency is also observed at the EGFR substrate level. Shc adaptor proteins are well-characterized adaptor proteins linking the EGFR to activation of the Ras/Raf/ERK-MAPK signaling cascade. As shown in Fig. 3B, both Crm197 and BB94 pretreatment of Cos-7 cells strongly suppressed stress-induced Shc tyrosine phosphorylation, which matches that of the EGFR itself. Therefore, phosphorylation of Shc by stress stimuli critically depends on a ligand-dependent EGFR phosphorylation mechanism in Cos-7 cells.

Ectodomain shedding of pro-HB-EGF is induced in response to osmotic and oxidative stress in Cos-7 cells. To further substantiate the role of HB-EGF in this ligand-dependent EGFR stimulation mechanism, we directly investigated pro-HB-EGF processing by flow cytometric analysis of the amount of ligand precursor present on the cell surface of Cos-7 cells before and after stimulation with sorbitol or hydrogen peroxide. As shown in Fig. 4A, both stimuli lead to a rapid reduction of HB-EGF precursor detectable on the cell surface which is comparable to the decrease observed in response to EGFR
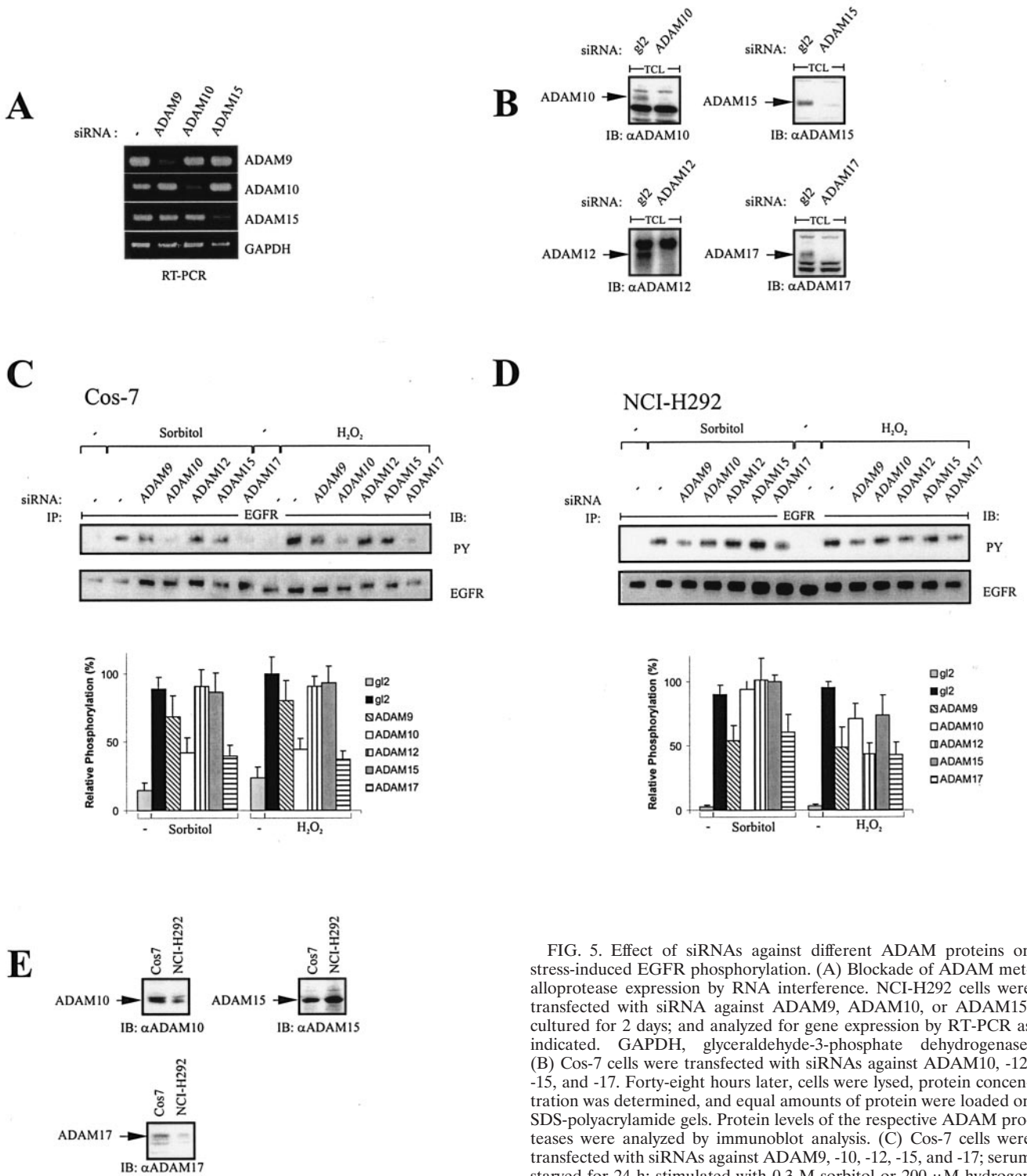
FIG. 5. Effect of siRNAs against different ADAM proteins on stress-induced EGFR phosphorylation. (A) Blockade of ADAM met-alloprotease expression by RNA interference. NCI-H292 cells were transfected with siRNA against ADAM9, ADAM10, or ADAM15; cultured for 2 days; and analyzed for gene expression by RT-PCR as indicated. GAPDH, glyceraldehyde-3-phosphate dehydrogenase. (B) Cos-7 cells were transfected with siRNAs against ADAM10, -12, -15, and -17. Forty-eight hours later, cells were lysed, protein concentration was determined, and equal amounts of protein were loaded on SDS-polyacrylamide gels. Protein levels of the respective ADAM proteases were analyzed by immunoblot analysis. (C) Cos-7 cells were transfected with siRNAs against ADAM9, -10, -12, -15, and -17; serum starved for 24 h; stimulated with 0.3 M sorbitol or 200 μM hydrogen peroxide for 10 min; and assayed for EGFR tyrosine phosphorylation content. Data from three independent experiments were quantified with the Fuji LAS1000 imaging system. (D) NCI-H292 cells were treated as described for panel C. (E) Cos-7 and NCI-H292 cells were lysed, and expression of ADAM10, -15, and -17 was assessed by immunoblot analysis as described for panel B.
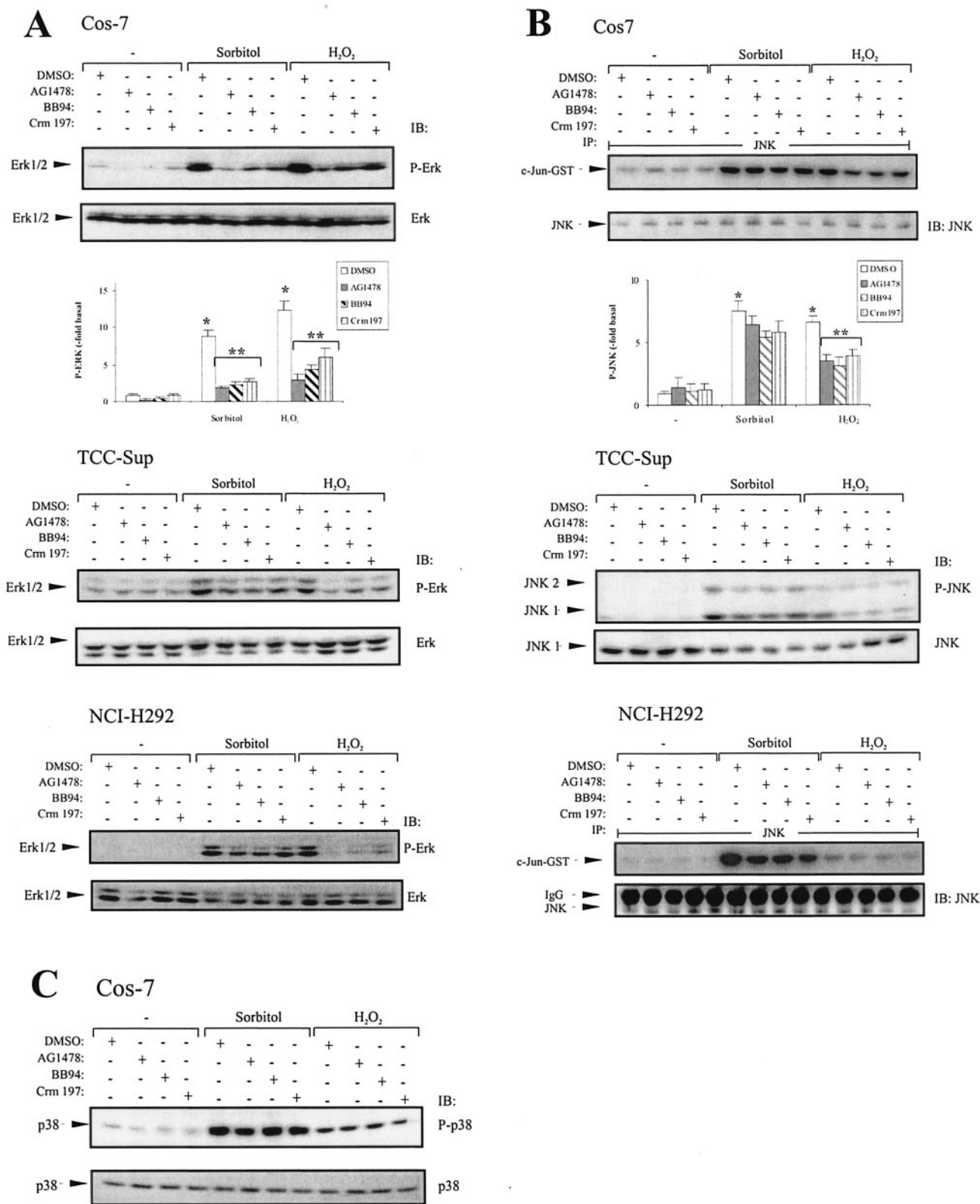
FIG. 6. MAPK activation in response to stress agents and blockade of EGFR, metalloprotease, and HB-EGF function. (A) Cos-7 cells transiently transfected with pcDNA3-HA-ERK2 and TCC-Sup and NCI-H292 cells were pretreated with AG1478 (250 nM), BB94 (10 μM), Crm197 (10 μg/ml), or an equal volume of empty vehicle (dimethyl sulfoxide [DMSO]) for 20 min and stimulated with 0.3 M sorbitol or 200 μM hydrogen peroxide for 30 min. After cell lysis total lysates were immunoblotted with anti-phospho-ERK antibody, followed by reprobing of the same membranes with polyclonal anti-ERK antibody. Quantitative analysis of ERK phosphorylation from three independent experiments (means ± standard deviations) was performed with the Fuji LAS1000 imaging system. *, $P < 0.001$ for control versus stimulation; **, $P < 0.006$ for

signal transactivation (21, 38). Moreover, in accordance with the results presented in Fig. 3A, pretreatment with the metalloprotease inhibitor BB94 abolished pro-HB-EGF processing. In addition to the disappearance of HB-EGF precursor, we used Cos-7 cells ectopically expressing pro-HB-EGF to determine the amount of mature soluble HB-EGF released from the cell surface into the cell culture medium. As shown in Fig. 4B, treatment with either sorbitol or hydrogen peroxide induced an increase of HB-EGF in the cell culture supernatant as determined by immunoblot analysis. Again, HB-EGF release was blocked by preincubation with the metalloprotease inhibitor BB94, confirming the involvement of a metalloprotease.

Metalloproteases of the ADAM family mediate EGFR activation by osmotic and oxidative stress. The finding that metalloprotease-dependent mechanisms significantly contribute to stress-induced EGFR and Shc activation raised the question of which metalloprotease(s) is involved. We used the RNA interference technique to specifically inhibit the endogenous expression of the ADAM proteases ADAM9, -10, -12, -15, and -17, which have already been implicated in EGF-like ligand release (1, 23, 36, 47, 54). Figure 5A shows the efficient and specific knockdown of target gene expression by the siRNAs against ADAM9, -10, and -15 shown by RT-PCR analysis. The corresponding knockdown of ADAM10, -12, -15, and -17 is demonstrated by Western blot analysis (Fig. 5B). The siRNAs against ADAM12 and -17 have been described previously (21). Transient transfection of these siRNAs directed against the individual proteases and subsequent phosphotyrosine analysis of the EGFR upon stimulation with either sorbitol or hydrogen peroxide revealed that ADAM10, ADAM17, and to a lesser extent ADAM9 are involved in EGFR activation in response to both stress stimuli in Cos-7 cells (Fig. 5C). Since we were particularly interested in the regulation of these processes in human cancer cells, we further investigated the involvement of ADAM family members in the lung carcinoma cell line NCI-H292. Similar to the results obtained in Cos-7 cells, ADAM17 also mediates the stress-induced EGFR activation, as demonstrated in Fig. 5D. But, in contrast to Cos-7 cells, ADAM10 is not involved in the stress response of NCI-H292 cells, while ADAM9 has a distinct role in this signaling context. To address the question whether differences in the relative expression levels of ADAM10 in Cos-7 and NCI-H292 cells account for the observed differential contributions to the signaling mechanism, we used cDNA macroarrays to analyze the different mRNA levels of ADAM9, -10, -12, -15, and -17 in Cos-7 and NCI-H292 cells. Different mRNA levels were found for ADAM10 and ADAM17 (data not shown) and verified by immunoblot analysis (Fig. 5E). ADAM17, which participates in both Cos-7 and NCI-H292 stress-induced EGFR activation,

is expressed at higher levels in Cos-7 than in NCI-H292 cells. However, the same expression pattern can be seen in the case of ADAM10, which is not involved in HB-EGF processing in NCI-H292 cells in response to stress. Thus, these observations suggest that the different contributions of ADAM proteins to the stress-induced EGFR activation are largely independent of their relative expression levels.

Taken together, cell-type-specific but overlapping sets of ADAM family members regulate HB-EGF-dependent EGFR activation in response to stress agents.

Activation of the MAPKs ERK1/2 and JNK in response to hyperosmolarity and oxidative stress is mediated by HB-EGF-dependent EGFR activation. Since the MAPKS ERK1/2 and JNK are activated by hypertonicity and ROS (13, 31), we asked whether the ligand-dependent EGFR phosphorylation contributes to the induction of these MAPK family members by stress stimuli. To investigate the overall dependence of stress-induced MAPK activation on the EGFR kinase activity, we used the selective EGFR blocker AG1478. Furthermore, we compared the effects of tyrosine kinase inhibition with the suppression of ligand-dependent EGFR activation by BB94 and Crm197. As shown in Fig. 6A (upper panel), both sorbitol and hydrogen peroxide significantly induced activation of ERK1/2, which is blocked by AG1478. Moreover, BB94 and Crm197 are almost as effective in blocking ERK1/2 phosphorylation. These data suggest that stress-induced ERK1/2 activation in Cos-7 cells almost completely depends on EGFR activation, which can be largely attributed to a ligand-dependent mechanism. The same experimental setup was used to address the question whether the same mechanistic concept is valid for stress signaling in human carcinoma cell lines. As shown in Fig. 6A, we found that hyperosmolarity- and oxidative stress-induced ERK1/2 activation in TCC-Sup and NCI-H292 cells was substantially blocked by AG1478, BB94, or Crm197 (Fig. 6A, middle and lower panels). Interestingly, although oxidative stress induces EGFR phosphorylation only partially through a ligand-dependent mechanism in NCI-H292 cells, ERK activation depends mainly on pro-HB-EGF processing in this cell type.

In addition to ERK1/2, we were interested in the signaling mechanisms leading to activation of JNK MAPKs. Figure 6B (upper panel) shows the JNK activity induced by osmotic and oxidative stress upon pretreatment with AG1478, BB94, or Crm197. While sorbitol-induced JNK activity is largely independent of the EGFR in Cos-7 cells, 50% of the oxidative stress-induced JNK activity significantly depends on EGFR and HB-EGF. Similar results were obtained in the bladder carcinoma cell line TCC-Sup as shown in Fig. 6B (middle panel). In contrast, hydrogen peroxide-stimulated JNK activation in the lung carcinoma cell line NCI-H292 appears to be

---

stimulation versus stimulation plus inhibitors. (B) Cos-7 and NCI-H292 cells were treated as described for panel A. After lysis, JNK was immunoprecipitated using an anti-JNK antibody, and JNK activity was assayed using GST–c-JUN fusion protein as a substrate. Phosphorylated GST–c-JUN was visualized by autoradiography, and JNK was immunoblotted in parallel using polyclonal JNK antibody. Quantitative analysis of GST–c-JUN phosphorylation from three independent experiments (means ± standard deviations) was performed with the Fuji LAS1000 imaging system. *, $P < 0.001$ for control versus stimulation; **, $P < 0.01$ for H_2O_2 stimulation versus H_2O_2 plus inhibitors. TCC-Sup cells were treated as described for panel A. After cell lysis, JNK phosphorylation was assayed by immunoblotting cell extracts with anti-phospho-JNK antibody and the same filters were reprobed with anti-JNK antibody. (C) p38 phosphorylation is independent of EGFR, metalloprotease, and HB-EGF function. Cos-7 cells were treated as described for panel A. p38 phosphorylation was assayed by immunoblotting cell extracts with anti-phospho-p38 antibody and reprobing the same filters with anti-p38 antibody.
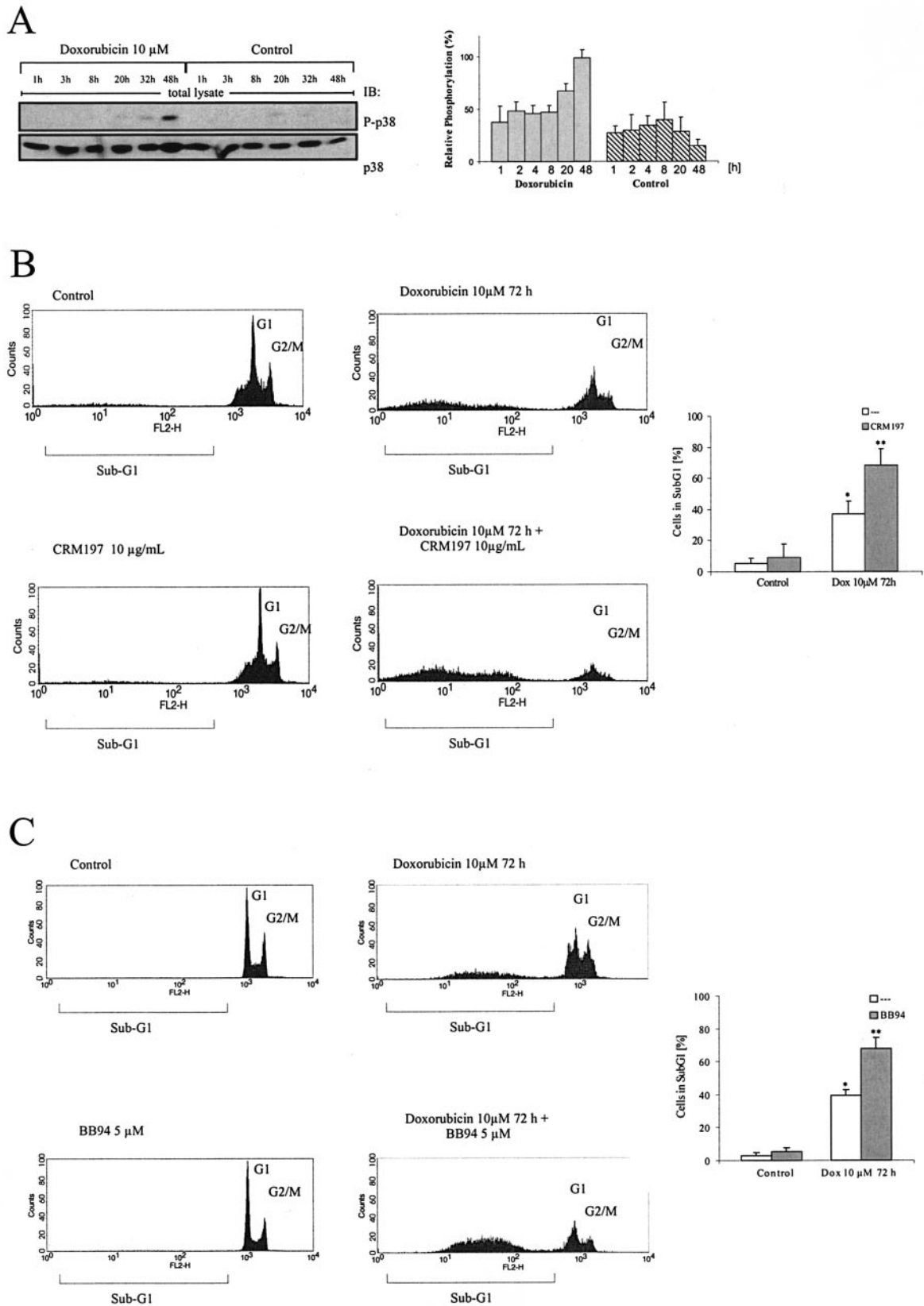
FIG. 7. Doxorubicin-induced cell death of TCC-Sup carcinoma cells. (A) p38 activation in response to doxorubicin treatment. TCC-Sup cells were seeded and treated with doxorubicin for the indicated time points. After cell lysis, p38 activation was assessed by immunoblotting cell extracts with anti-phospho-p38 antibody and reprobing the same filters with anti-p38 antibody. Data from three independent experiments were quantified

independent of the EGFR, while JNK activity in response to hypertonicity partially depends on a ligand-dependent EGFR activation pathway. In agreement with the finding that p38 acts as an upstream mediator of stress-induced EGFR activation (Fig. 2), p38 activity depended neither on the EGFR kinase activity nor on metalloprotease or HB-EGF function in Cos-7 cells (Fig. 6C).

Blockade of HB-EGF function strongly enhances doxorubicin-induced cell death. Treatment of tumor cells with chemotherapeutics has been shown to activate the stress kinases p38 and JNK (2). Similar results with respect to p38 activation were obtained with TCC-Sup bladder carcinoma cells after exposure to the chemotherapeutic agent doxorubicin (Fig. 7A). In this physiological context, p38-triggered pro-HB-EGF processing and subsequent EGFR activation might provide a cellular survival signal and thereby counteract doxorubicin-induced apoptosis. To test this hypothesis, we treated TCC-Sup cells with the specific HB-EGF blocker Crm197 and measured its effect on doxorubicin-induced cell death. Remarkably, Crm197 treatment significantly enhanced the apoptotic response to doxorubicin compared to that for doxorubicin alone, while Crm197 had only a minor effect on cell survival (Fig. 7B). This synergistic effect was also observed when cells were treated with doxorubicin and the metalloprotease inhibitor BB94. Thus, these results point to a physiological significance of p38-dependent EGFR activation involving metalloprotease-mediated pro-HB-EGF processing as a pathway employed by tumor cells to evade apoptosis upon exposure to chemotherapeutic agents.

DISCUSSION

How mammalian cells respond to physical stress has been intensely studied, but despite these extensive research efforts, various mechanistic aspects of stress-induced signaling have remained elusive (2, 18, 27, 31). Our present study provides new insights into growth factor-dependent mechanisms leading to EGFR and subsequent MAPK activation in response to osmotic and oxidative stress in human carcinoma cells.

We have provided various lines of direct evidence demonstrating that EGFR phosphorylation induced by both osmotic and oxidative stress requires a metalloprotease activity triggering the release of mature HB-EGF in Cos-7 cells and human carcinoma cell lines. Our findings significantly extend results from earlier reports, which indicated a role of mechanisms such as receptor aggregation, phosphatase inactivation, or the stimulation of intracellular kinases in stress-induced EGFR activation (4, 30, 41). These previously described mechanisms might contribute to the partially ligand-independent EGFR phosphorylation in NCI-H292 cells, whereas a ligand-dependent activation fully accounts for receptor phosphorylation by osmotic and oxidative stress in Cos-7 and TCC-Sup bladder carcinoma cells. Thus, the respective contribution of different

routes leading to EGFR activation appears to depend on the cellular context. It is noteworthy that Chen et al. (8) attributed the hydrogen peroxide-induced EGFR activation in Cos-7 cells to a ligand-independent mechanism involving c-Src. In contrast to these earlier observations, we did not achieve inhibition of EGFR activation by oxidative stress with the Src inhibitors PP1 and PP2 in the same cell system (unpublished data).

Stress-induced signaling might also trigger a positive feedback loop, further enhancing ligand-dependent EGFR activation, since previous investigations revealed stress-induced expression of HB-EGF and amphiregulin (35). Interestingly, Zenz et al. demonstrated a functional correlation among c-Jun, a downstream target of the JNK family; the EGFR; and HB-EGF, as in c-Jun-deficient keratinocytes both HB-EGF and EGFR expression levels were reduced (55).

Although Frank et al. recently implicated HB-EGF in hydrogen peroxide-induced EGFR phosphorylation in vascular smooth muscle cells (19), the various components involved in this process have not been defined. We provide the first experimental evidence that ADAM proteases are responsible for shedding of pro-HB-EGF upon cellular stress. Interestingly, while GPCR-mediated EGFR transactivation occurs through distinct individual ADAM proteases (21, 54), we found that two or more ADAM proteases become active upon cellular stress. ADAM17 appears to be generally involved in stress-stimulated shedding events, while ADAM9, ADAM10, and ADAM12 also can contribute to different extents depending on the cell system and type of stimulus. All of these enzymes have been previously implicated in EGF-like ligand shedding (1, 23, 24, 32, 54). Our identification of stress-induced ADAM family members distinct from those regulated through GPCRs is corroborated by previous reports demonstrating that ADAM9 cleaves pro-HB-EGF in response to tetradecanoyl phorbol acetate (TPA) stimulation in VeroH cells (23), while in the same cellular system pro-HB-EGF processing after LPA stimulation is independent of ADAM9 (51). However, the relative contribution of the different ADAM proteases seems to be independent of their quantitative presence in cells (Fig. 5E). Taken together, these data suggest that pro-HB-EGF sheddases are defined by both the cellular context and the stimulus. Moreover, ADAM9-knockout mice lack an obvious phenotype and ADAM9$^{-/-}$ fibroblasts display no defects in pro-HB-EGF processing (52), which strongly argues for functional redundancy among pro-HB-EGF-cleaving enzymes in vivo.

How are the metalloproteases of the ADAM family activated, finally leading to EGFR phosphorylation and downstream signaling responses? Previous reports demonstrated regulation of metalloprotease-mediated ectodomain cleavage of transmembrane proteins in response to growth factors and TPA by the MAPKs ERK1/2, while the basal level of ectodomain shedding has been attributed to p38 activity (15, 20, 40).

with the Fuji LAS1000 imaging system. (B) Blockade of HB-EGF function enhances cell death in response to doxorubicin. Cells were treated for 72 h with 10 μM doxorubicin and 10 μg of Crm197/ml every 24 h as indicated. After collection of cells in assay buffer, nuclei were stained with propidium iodide and analyzed by flow cytometric analysis. Data from four independent experiments (means ± standard deviations) were quantified. *, $P < 0.001$ for control versus doxorubicin; **, $P < 0.004$ for doxorubicin versus doxorubicin plus Crm197. (C) Blockade of metalloprotease function enhances cell death in response to doxorubicin. Cells were treated and analyzed as described for panel B except that BB94 (5 μM) was used instead of Crm197. *, $P < 0.003$ for control versus doxorubicin; **, $P < 0.007$ for doxorubicin versus doxorubicin plus BB94.

Moreover, p38 has been implicated as an upstream mediator of the EGFR in the sorbitol-induced EGFR activation in human nontransformed keratinocytes (10). In contrast to our results, the authors of that report excluded a ligand-dependent mechanism based on medium transfer experiments. As the released EGF-like ligand may be retained in the extracellular matrix through binding to heparan sulfate proteoglycans (38), an involvement of ligand-dependent EGFR activation cannot be ruled out by this type of experimental approach. These reports and the finding that p38 activity in our systems is independent of the EGFR phosphorylation state prompted us to ask whether stress-activated p38 is the upstream signaling element that controls ligand-dependent EGFR activation. Indeed, we found that preincubation with a specific p38 inhibitor eliminated stress-induced EGFR activation, while blocking ERK1/2 activation left EGFR phosphorylation unaffected. In contrast, p38 activation itself in response to stress agents is independent of the EGFR as assessed by use of the EGFR selective inhibitor AG1478. Furthermore, time course experiments revealed that p38 activation precedes EGFR phosphorylation, which is a necessary prerequisite for p38 being located upstream of the EGFR, while ERK1/2 and JNK activation occurs even later. Together, these data suggest p38 as the upstream inducer of ligand-dependent EGFR activation and its subsequent downstream signaling. These results are in good agreement with the report by Takenobu et al. demonstrating p38-controlled shedding of pro-HB-EGF (49). Ruano et al. proposed in a recent publication the existence of a p38-controlled phosphotyrosine phosphatase, which becomes inactivated upon p38 stimulation, leading to EGFR phosphorylation (42). Since the researchers used unusually high concentrations and a very short time of incubation of the p38 inhibitor, these data do not exclude a ligand-dependent EGFR activation mechanism.

Activation of ERK1/2 and JNK in response to oxidative and osmotic stress represents an important step in the cellular stress response (reviewed in reference 31). Stress signaling via MAPKs is often increased in cancer cells, which frequently produce high levels of ROS per se (6, 48). Moreover, anticancer drugs or radiation therapy can further activate stress signaling cascades (2), which has also been attributed to the production of ROS caused by these agents. Here, we show that the stress-induced ligand-dependent EGFR activation is a prerequisite for subsequent ERK1/2 and, to a lesser extent, also JNK MAPK activation (Fig. 6). As ligand-dependent, EGFR-mediated MAPK signaling can control cell survival through induction of apoptosis regulators such as the Bcl-2 family (26), it might also play a role in the protection of bladder carcinoma cells from doxorubicin-induced apoptosis observed in our experiments. Consistent with this hypothesis, blockade of HB-EGF or metalloprotease function strongly enhanced doxorubicin-induced cell death (Fig. 7). As chemotherapeutic agents have been previously shown to activate stress signaling cascades (2, 33, 43), this signaling mechanism provides a molecular explanation for the ability of tumor cells to evade drug-induced cell death.

Increasing evidence implicates particularly ROS-induced oxidative stress in a variety of human disorders as diverse as cardiovascular, neurodegenerative, and hyperproliferative diseases and cancer. Therefore, our results are of special significance for the understanding of pathophysiological disorders and the development of respective therapeutic approaches.

Our findings emphasize the importance of ADAM family proteases and HB-EGF as critical mediators of the stress response in human cancer cells and suggest that cross-communication between different groups of MAPKs employs ADAM proteases and the EGFR as signaling intermediates. Future work will be necessary to substantiate the broad significance of the mechanisms elucidated here and to develop targeted cancer therapies on the basis of our findings.

REFERENCES

1. **Asakura, M., M. Kitakaze, S. Takashima, Y. Liao, F. Ishikura, T. Yoshinaka, H. Ohmoto, K. Node, K. Yoshino, H. Ishiguro, H. Asanuma, S. Sanada, Y. Matsumura, H. Takeda, S. Beppu, M. Tada, M. Hori, and S. Higashiyama.** 2002. Cardiac hypertrophy is inhibited by antagonism of ADAM12 processing of HB-EGF: metalloproteinase inhibitors as a new therapy. Nat. Med. **8:**35–40.
2. **Benhar, M., D. Engelberg, and A. Levitzki.** 2002. ROS, stress-activated kinases and stress signaling in cancer. EMBO Rep. **3:**420–425.
3. **Biscardi, J. S., M. C. Maa, D. A. Tice, M. E. Cox, T. H. Leu, and S. J. Parsons.** 1999. c-Src-mediated phosphorylation of the epidermal growth factor receptor on Tyr845 and Tyr1101 is associated with modulation of receptor function. J. Biol. Chem. **274:**8335–8343.
4. **Blanchetot, C., L. G. J. Tertoolen, and J. den Hertog.** 2002. Regulation of receptor protein-tyrosine phosphatase {alpha} by oxidative stress. EMBO J. **21:**493–503.
5. **Borrell-Pages, M., F. Rojo, J. Albanell, J. Baselga, and J. Arribas.** 2003. TACE is required for the activation of the EGFR by TGF-alpha in tumors. EMBO J. **22:**1114–1124.
6. **Burdon, R. H.** 1995. Superoxide and hydrogen peroxide in relation to mammalian cell proliferation. Free Radic. Biol. Med. **18:**775–794.
7. **Carpenter, G.** 1999. Employment of the epidermal growth factor receptor in growth factor-independent signaling pathways. J. Cell Biol. **146:**697–702.
8. **Chen, K., J. A. Vita, B. C. Berk, and J. F. Keaney, Jr.** 2001. c-Jun N-terminal kinase activation by hydrogen peroxide in endothelial cells involves SRC-dependent epidermal growth factor receptor transactivation. J. Biol. Chem. **276:**16045–16050.
9. **Chen, Z., T. B. Gibson, F. Robinson, L. Silvestro, G. Pearson, B. Xu, A. Wright, C. Vanderbilt, and M. H. Cobb.** 2001. MAP kinases. Chem. Rev. **101:**2449–2476.
10. **Cheng, H., J. Kartenbeck, K. Kabsch, X. Mao, M. Marques, and A. Alonso.** 2002. Stress kinase p38 mediates EGFR transactivation by hyperosmolar concentrations of sorbitol. J. Cell. Physiol. **192:**234–243.
11. **Daub, H., C. Wallasch, A. Lankenau, A. Herrlich, and A. Ullrich.** 1997. Signal characteristics of G protein-transactivated EGF receptor. EMBO J. **16:**7032–7044.
12. **Daub, H., F. U. Weiss, C. Wallasch, and A. Ullrich.** 1996. Role of transactivation of the EGF receptor in signalling by G-protein-coupled receptors. Nature **379:**557–560.
13. **de Nadal, E., P. M. Alepuz, and F. Posas.** 2002. Dealing with osmostress through MAP kinase activation. EMBO Rep. **3:**735–740.
14. **Diaz-Rodriguez, E., J. C. Montero, A. Esparis-Ogando, L. Yuste, and A. Pandiella.** 2002. Extracellular signal-regulated kinase phosphorylates tumor necrosis factor alpha-converting enzyme at threonine 735: a potential role in regulated shedding. Mol. Biol. Cell **13:**2031–2044.
14a.**Elbashir, S. M., J. Harborth, W. Lendeckel, A. Yalcin, K. Weber, and T. Tuschl.** 2001. Duplexes of 21-nucleotide RNAs mediate RNA interference in cultured mammalian cells. Nature **411:**494–498.
15. **Fan, H., and R. Derynck.** 1999. Ectodomain shedding of TGF-alpha and other transmembrane proteins is induced by receptor tyrosine kinase activation and MAP kinase signaling cascades. EMBO J. **18:**6962–6972.
16. **Fan, H., C. W. Turck, and R. Derynck.** 2003. Characterization of growth factor-induced serine phosphorylation of tumor necrosis factor-alpha converting enzyme (TACE) and of an alternatively translated polypeptide. J. Biol. Chem. **278:**18617–18627.
17. **Finkel, T.** 1998. Oxygen radicals and signaling. Curr. Opin. Cell Biol. **10:**248–253.
18. **Finkel, T., and N. J. Holbrook.** 2000. Oxidants, oxidative stress and the biology of ageing. Nature **408:**239–247.

19. **Frank, G. D., M. Mifune, T. Inagami, M. Ohba, T. Sasaki, S. Higashiyama, P. J. Dempsey, and S. Eguchi.** 2003. Distinct mechanisms of receptor and nonreceptor tyrosine kinase activation by reactive oxygen species in vascular smooth muscle cells: role of metalloprotease and protein kinase C-δ. Mol. Cell. Biol. **23:**1581–1589.

20. **Gechtman, Z., J. L. Alonso, G. Raab, D. E. Ingber, and M. Klagsbrun.** 1999. The shedding of membrane-anchored heparin-binding epidermal-like growth factor is regulated by the Raf/mitogen-activated protein kinase cascade and by cell adhesion and spreading. J. Biol. Chem. **274:**28828–28835.

21. **Gschwind, A., S. Hart, O. M. Fischer, and A. Ullrich.** 2003. TACE cleavage of proamphiregulin regulates GPCR-induced proliferation and motility of cancer cells. EMBO J. **22:**2411–2421.

22. **Gschwind, A., N. Prenzel, and A. Ullrich.** 2002. Lysophosphatidic acid-induced squamous cell carcinoma cell proliferation and motility involves epidermal growth factor receptor signal transactivation. Cancer Res. **62:**6329–6336.

23. **Izumi, Y., M. Hirata, H. Hasuwa, R. Iwamoto, T. Umata, K. Miyado, Y. Tamai, T. Kurisaki, A. Sehara-Fujisawa, S. Ohno, and E. Mekada.** 1998. A metalloprotease-disintegrin, MDC9/meltrin-gamma/ADAM9 and PKCdelta are involved in TPA-induced ectodomain shedding of membrane-anchored heparin-binding EGF-like growth factor. EMBO J. **17:**7260–7272.

24. **Jackson, L. F., T. H. Qiu, S. W. Sunnarborg, A. Chang, C. Zhang, C. Patterson, and D. C. Lee.** 2003. Defective valvulogenesis in HB-EGF and TACE-null mice is associated with aberrant BMP signaling. EMBO J. **22:**2704–2716.

25. **Johnson, G. L., and R. Lapadat.** 2002. Mitogen-activated protein kinase pathways mediated by ERK, JNK, and p38 protein kinases. Science **298:**1911–1912.

26. **Jost, M., T. M. Huggett, C. Kari, L. H. Boise, and U. Rodeck.** 2001. Epidermal growth factor receptor-dependent control of keratinocyte survival and Bcl-xL expression through a MEK-dependent pathway. J. Biol. Chem. **276:**6320–6326.

27. **Kamata, H., and H. Hirata.** 1999. Redox regulation of cellular signalling. Cell. Signal. **11:**1–14.

28. **Keates, S., S. Sougioultzis, A. C. Keates, D. Zhao, R. M. Peek, Jr., L. M. Shaw, and C. P. Kelly.** 2001. *cag*+ *Helicobacter pylori* induce transactivation of the epidermal growth factor receptor in AGS gastric epithelial cells. J. Biol. Chem. **276:**48127–48134.

29. **King, C. R., I. Borrello, L. Porter, P. Comoglio, and J. Schlessinger.** 1989. Ligand-independent tyrosine phosphorylation of EGF receptor and the erbB-2/neu proto-oncogene product is induced by hyperosmotic shock. Oncogene **4:**13–18.

30. **Knebel, A., H. Rahmsdorf, A. Ullrich, and P. Herrlich.** 1996. Dephosphorylation of receptor tyrosine kinases as target of regulation by radiation, oxidants or alkylating agents. EMBO J. **15:**5314–5325.

31. **Kyriakis, J. M., and J. Avruch.** 2001. Mammalian mitogen-activated protein kinase signal transduction pathways activated by stress and inflammation. Physiol. Rev. **81:**807–869.

32. **Lemjabbar, H., and C. Basbaum.** 2002. Platelet-activating factor receptor and ADAM10 mediate responses to *Staphylococcus aureus* in epithelial cells. Nat. Med. **8:**41–46.

33. **Losa, J. H., C. P. Cobo, J. G. Viniegra, V. J. Lobo, S. R. Cajal, and R. Sanchez-Prieto.** 2003. Role of the p38 MAPK pathway in cisplatin-based therapy. Oncogene **22:**3998–4006.

34. **Merlos-Suarez, A., S. Ruiz-Paz, J. Baselga, and J. Arribas.** 2001. Metalloprotease-dependent protransforming growth factor-alpha ectodomain shedding in the absence of tumor necrosis factor-alpha-converting enzyme. J. Biol. Chem. **276:**48510–48517.

35. **Miyazaki, Y., S. Hiraoka, S. Tsutsui, S. Kitamura, Y. Shinomura, and Y. Matsuzawa.** 2001. Epidermal growth factor receptor mediates stress-induced expression of its ligands in rat gastric epithelial cells. Gastroenterology **120:**108–116.

36. **Peschon, J. J., J. L. Slack, P. Reddy, K. L. Stocking, S. W. Sunnarborg, D. C. Lee, W. E. Russell, B. J. Castner, R. S. Johnson, J. N. Fitzner, R. W. Boyce, N. Nelson, C. J. Kozlosky, M. F. Wolfson, C. T. Rauch, D. P. Cerretti, R. J. Paxton, C. J. March, and R. A. Black.** 1998. An essential role for ectodomain shedding in mammalian development. Science **282:**1281–1284.

37. **Prenzel, N., O. M. Fischer, S. Streit, S. Hart, and A. Ullrich.** 2001. The epidermal growth factor receptor family as a central element for cellular signal transduction and diversification. Endocr. Relat. Cancer **8:**11–31.

38. **Prenzel, N., E. Zwick, H. Daub, M. Leserer, R. Abraham, C. Wallasch, and A. Ullrich.** 1999. EGF receptor transactivation by G-protein-coupled receptors requires metalloproteinase cleavage of proHB-EGF. Nature **402:**884–888.

39. **Rao, G. N.** 1996. Hydrogen peroxide induces complex formation of SHC-Grb2-SOS with receptor tyrosine kinase and activates Ras and extracellular signal-regulated protein kinases group of mitogen-activated protein kinases. Oncogene **13:**713–719.

40. **Rizoli, S. B., O. D. Rotstein, and A. Kapus.** 1999. Cell volume-dependent regulation of L-selectin shedding in neutrophils. A role for p38 mitogen-activated protein kinase. J. Biol. Chem. **274:**22072–22080.

41. **Rosette, C., and M. Karin.** 1996. Ultraviolet light and osmotic stress: activation of the JNK cascade through multiple growth factor and cytokine receptors. Science **274:**1194–1197.

42. **Ruano, M. J., S. Hernandez-Hernando, A. Jimenez, C. Estrada, and A. Villalobo.** 2003. Nitric oxide-induced epidermal growth factor-dependent phosphorylations in A431 tumour cells. Eur. J. Biochem. **270:**1828–1837.

43. **Sanchez-Prieto, R., J. M. Rojas, Y. Taya, and J. S. Gutkind.** 2000. A role for the p38 mitogen-activated protein kinase pathway in the transcriptional activation of p53 on genotoxic stress by chemotherapeutic agents. Cancer Res. **60:**2464–2472.

44. **Schägger, H., and G. von Jargow.** 1987. Tricine-sodium dodecyl sulfate-polyacrylamide gel electrophoresis for the separation of proteins in the range from 1 to 100 kDa. Anal. Biochem. **166:**368–379.

45. **Schlessinger, J.** 2002. Ligand-induced, receptor-mediated dimerization and activation of EGF receptor. Cell **110:**669–672.

46. **Sudo, T., and M. Karin.** 2000. Assays for JNK and p38 mitogen-activated protein kinases. Methods Enzymol. **322:**388–392.

47. **Sunnarborg, S. W., C. L. Hinkle, M. Stevenson, W. E. Russell, C. S. Raska, J. J. Peschon, B. J. Castner, M. J. Gerhart, R. J. Paxton, R. A. Black, and D. C. Lee.** 2002. Tumor necrosis factor-alpha converting enzyme (TACE) regulates epidermal growth factor receptor ligand availability. J. Biol. Chem. **277:**12838–12845.

48. **Szatrowski, T. P., and C. F. Nathan.** 1991. Production of large amounts of hydrogen peroxide by human tumor cells. Cancer Res. **51:**794–798.

49. **Takenobu, H., A. Yamazaki, M. Hirata, T. Umata, and E. Mekada.** 2003. The stress- and inflammatory cytokine-induced ectodomain shedding of heparin-binding epidermal growth factor-like growth factor is mediated by p38 MAPK, distinct from the 12-O-tetradecanoylphorbol-13-acetate- and lysophosphatidic acid-induced signaling cascade. J. Biol. Chem. **278:**17255–17262.

50. **Tice, D. A., J. S. Biscardi, A. L. Nickles, and S. J. Parsons.** 1999. Mechanism of biological synergy between cellular Src and epidermal growth factor receptor. Proc. Natl. Acad. Sci. USA **96:**1415–1420.

51. **Umata, T., M. Hirata, T. Takahashi, F. Ryu, S. Shida, Y. Takahashi, M. Tsuneoka, Y. Miura, M. Masuda, Y. Horiguchi, and E. Mekada.** 2001. A dual signaling cascade that regulates the ectodomain shedding of heparin-binding epidermal growth factor-like growth factor. J. Biol. Chem. **276:**30475–30482.

52. **Weskamp, G., H. Cai, T. A. Brodie, S. Higashiyama, K. Manova, T. Ludwig, and C. P. Blobel.** 2002. Mice lacking the metalloprotease-disintegrin MDC9 (ADAM9) have no evident major abnormalities during development or adult life. Mol. Cell. Biol. **22:**1537–1544.

53. **Yamauchi, T., K. Ueki, K. Tobe, H. Tamemoto, N. Sekine, M. Wada, M. Honjo, M. Takahashi, T. Takahashi, H. Hirai, T. Tushima, Y. Akanuma, T. Fujita, I. Komuro, Y. Yazaki, and T. Kadowaki.** 1997. Tyrosine phosphorylation of the EGF receptor by the kinase Jak2 is induced by growth hormone. Nature **390:**91–96.

54. **Yan, Y., K. Shirakabe, and Z. Werb.** 2002. The metalloprotease Kuzbanian (ADAM10) mediates the transactivation of EGF receptor by G protein-coupled receptors. J. Cell Biol. **158:**221–226.

55. **Zenz, R., H. Scheuch, P. Martin, C. Frank, R. Eferl, L. Kenner, M. Sibilia, and E. F. Wagner.** 2003. c-Jun regulates eyelid closure and skin tumor development through EGFR signaling. Dev. Cell **4:**879–889.